Journal of the Serbian Chemical Society
JSCS-info@shd.org.rs • www.shd.org.rs/JSCS

J. Serb. Chem. Soc. *78* (11) 1641–1654 (2013)
JSCS–4524

UDC 616–008.854+54.351–039.7:
543.422.25+543.456
Original scientific paper

NMR microscopy of tissue in organic and mixed solvents

SLOBODAN MACURA[1]*, PRASANNA K. MISHRA[1], JEFFREY D. GAMEZ[2] and ISTVAN PIRKO[2]

[1]*Department of Biochemistry and Molecular Biology and* [2]*Department of Neurology, Mayo Clinic, Rochester, Minnesota, 55905, USA*

(Received 8 October 2013)

Abstract: The use organic and mixed solvents for nuclear magnetic resonance microscopy of fixed tissue is proposed as a means for improving image information content. NMR properties of some standard solvents (methanol, acetone or DMSO) and solvents in use for tissue processing in pathology (xylenes, paraffin, "Clearify") have been measured, reviewed and analyzed. It was found that DMSO and paraffin are very useful solvents that provide images of better quality than those obtained in water (neutralized formalin buffer). This is illustrated on formalin-fixed mouse brain sections imaged at 16.4 T (700 MHz).

Keywords: NMR, MRI, MRM, nuclear magnetic resonance, NMR imaging, NMR microscopy, magnetization transfer, cross-relaxation.

INTRODUCTION

Nuclear magnetic resonance (NMR) imaging,[1,2] in clinical settings known as magnetic resonance imaging (MRI),[3] is an indispensable tool in medicine providing non-invasively a detailed picture of tissues and organs in the human body. When performed on small samples with high spatial resolution, NMR imaging is frequently referred to as NMR microscopy.[4]

Proton (nucleus of hydrogen, ^{1}H) is most widely used nucleus in imaging because of its sensitivity and because of its abundance in tissue (water, carbohydrates, lipids and proteins). In most NMR images, only protons from water are observed since the human body is comprised of ≈60 % water. This translates into a water proton concentration of ≈65 M, whereas the concentration of any other proton (except fat) is below 1 M. In addition, protons built into macromolecules (proteins and carbohydrates) are not detectable under routine imaging conditions. Besides water, a strong proton signal can be detected from the aliphatic part of lipid chains (fat) but this can easily be suppressed (when needed) so that almost all clinical images are based on the detection of protons from tissue water.

* Corresponding author. E-mail: macura@mayo.edu
doi: 10.2298/JSC131108108M

Source of contrast in MRI

Compared to other imaging modalities (X-ray, ultrasound, positron emission, *etc*.), NMR has an extensive assortment of contrasting means, most of which are based on the molecular properties of water and their sensitivity to fine changes in molecular environment. For example, the T_1 relaxation rate of water is very sensitive to the presence of natural (deoxyhemoglobin) or artificial (paramagnetic ions, Gd^{3+}, Mn^{2+} and stable free radicals) paramagnetic centers. Paramagnetism of deoxyhemoglobin is the principal source of contrast in functional NMR imaging (fMRI), whereas the paramagnetism of different ions (Gd^{3+} and Mn^{2+}) represents the basis for the development of various contrast agents.[5] Similarly, the water T_2 relaxation depends on molecular mobility and the T_2* relaxation on the local magnetic susceptibility gradients. This dependence of water properties on local physicochemical environment led to the creation of dozens of NMR imaging methods that emphasize selected properties. The main purpose of developing new ways of imaging contrast is to discriminate different tissues (*e.g*., gray matter *vs*. white matter in the brain) or normal from diseased tissue (cancer, necrosis, plaques, *etc*.) in a unique and unambiguous way. However, the main problem is that under certain experimental conditions, contrast depends on several different properties simultaneously, which makes it difficult to attribute it to a single disease condition. Thus, it is desirable to understand the source of NMR contrast at the molecular level, which, due to interplay among numerous water/tissue interactions, is rather difficult.

Although the most important aspect of MRI is its application *in vivo,* NMR imaging of tissue or organs *ex vivo* is also of great value. The most obvious advantage of *ex vivo* imaging, compared to *in vivo*, is that it can be performed in more details due to the absence of motion and time restriction (typically less than an hour in human subject imaging). Imaging *ex vivo* could be performed with higher resolution and better contrast, and most importantly, could be correlated with other types of tissue analysis (histology) and thus could serve as a guide for interpreting *in vivo* images. *Ex vivo* imaging is performed on either fresh tissue (surgical specimens), or thawed tissue earlier preserved by deep freezing, or formalin-fixed (FF) tissue. In all cases, protons are detected from tissue water and thus, most of the ambiguities present *in vivo* are still present in *ex vivo* imaging. For example, spin echo attenuation of water protons depends simultaneously on water diffusion, chemical exchange with labile protons from tissue (proteins, polysaccharides or small metabolites), the presence of paramagnetic species *etc*., and individual contributions of various effects can be deduced only after a series of experiments.

Formalin-fixed (FF) tissue most frequently is subsequently embedded in paraffin for further histology (optical microscopy) analysis. In this process, tissue is exposed to a series of organic solvents (most frequently ethanol, xylenes) until it

is completely dehydrated. In clinical settings this is realized on almost every surgical specimen requiring histology analysis; thus, having tissue in an organic solvent is not a rarity. In this work, whether imaging tissue in an organic solvent has any advantages over imaging in water was investigated. The main expectation was that interactions of organic solvents with FF tissue are much simpler and that they could be influenced by the solvent composition. This could help to understand better the contribution of tissue water to contrast in different experiments. In addition, it is conceivable that suitable solvents or their mixture could selectively emphasize various tissue properties.

Water/tissue interactions

By interacting in various ways with structures and components of living systems, water acts as a solvent, reactant, lubricant, adhesive, transporter, *etc*. Thus, it is not surprising that the interaction of water with tissue was one of the first applications of NMR in biological systems.[6] For MRI and magnetic resonance spectroscopy (MRM), only fast interactions that affect the properties of bulk water are of interest. Then, the observed macroscopic property, R_{obs} (chemical shift, relaxation rates, diffusion rate, *etc*.), is an ensemble average of the properties of individual components, free R_f, and bound, R_b:

$$R_{obs} = f_f R_f + \sum_j \left(f_b R_b \right)_j \quad (1)$$

where f_f and f_b represent free and bound fractions, respectively, and

$$f_f + \sum_j \left(f_b \right)_j = 1$$

The summation goes over all species that represent water molecules in assumed bound states. For example, based on relaxation dispersion studies,[7] at least four different waters in proteins, *i.e*., surface, cavity, cleft, and metal water, could be identified. Water in each site may have its own mobility (rotational or translational) and may exchange protons within the site, among different sites, with bulk water or labile protein protons. Due to rapid exchange with bulk water,[8] all these sites and processes mediate properties of the observable bulk phase.[9] Thus, it is rather difficult to explain, on a molecular level, the principal sources of contrast in imaging experiments. For example, transverse relaxation of water in tissue can be equivalently described by two physically different models. One emphasizes the role of diffusion in a weak gradient of the magnetic field, and the other a chemical exchange between two proton sites in slightly different fields.[10] As both processes are likely to occur in water, it is hard to determine their individual contributions in any given case. However, the processes could be easily delineated if one could be quenched, which is feasible when water is replaced by a solvent without labile protons.

Organic solvent–tissue interaction

Tissue in an organic solvent is encountered quite frequently in research and clinical settings. Namely, for long-term preservation, tissue is treated with formalin and for pathology analysis treated with a series of solvents until it is finally embedded in paraffin. One reason for the present study was the wide availability of tissue in organic solvents. The other, perhaps more interesting, was the possibility of interpreting solvent tissue interactions on a molecular level. Most organic solvents neither dissociate nor react with tissue (after the tissue has been fixed), which significantly reduces the number of possible interactions. In addition, scanning the same specimen in different solvents could help better characterize NMR tissue properties relevant for imaging contrast.

Organic solvent–tissue interactions most likely depend on both the type of tissue and the solvent. A non-polar solvent may not interact with a tissue at all, whereas a polar solvent may interact preferentially with a polar fragment of tissue (polar protein side chains, polysaccharides, hydrophilic part of lipids, *etc*.), potentially distinguishing different types of tissue in a specimen.

Mixed solvent–tissue interaction

Preferential solvation, frequently observed in mixed solvent systems, is the preferential accumulation of one solvent component around a specific solute. Obviously, the degrees of solvation depend on all components involved. In the case of tissue imaging, preferential solvation could potentially serve as an additional means of contrasting: water could accumulate in hydrophilic regions whereas organic components could preferentially solvate the hydrophobic regions. In general, preferential solvation occurs on the molecular scale (one or more molecular layers) but in a highly packed tissue matrix, it is possible that it occur on a larger scale amenable to MRM. Moreover, mixed solvents could be useful for monitoring tissue–solvent interactions *via* the interligand nuclear Overhauser effect (ILOE).[11] The ILOE is observed if two ligands (in the present case solvent molecules) reside on the macromolecular surface (in the present case tissue) in close proximity longer than one nanosecond (for a process to be within the spin-diffusion limit[12]).

Solvent influence on the signal to noise ratio in MRM

The best image is the one that reveals a specimens microstructure without artifacts and maximal contrast and sensitivity. Besides the applied external magnetic field strength, B_0, hardware and method design, the quality of NMR images strongly depends on the chemical environment of the observed spins. Here, the properties of the imaging medium that could affect the image parameters are of most interest.

The signal to noise ratio (*SNR*) is proportional to the spin concentration *N*, and depends on the transverse relaxation time of the solvent, T_2*, and the imaginary part of the dielectric permittivity, ε″ as follows:[13]

$$SNR \propto N\sqrt{\frac{T_2 *}{\varepsilon''}} \tag{2}$$

The *SNR* also depends on the real part of the dielectric permittivity, ε′, but in a more complex way, with the general rule that the smaller the permittivity, the better is the *SNR*.[13] Thus, for a given tissue specimen, the *SNR* could be improved by selecting the solvent with the highest spin density, the longest T_2* relaxation time and smallest dielectric permittivity.

Similarly, an estimate of the experimental time, t_T, as a function of the desired signal to noise ratio SNR_D, and T_1 and T_2* relaxation times of the imaging medium can be obtained from the following equation:[14]

$$t_T \propto SNR_D^2 \frac{T_1}{T_2 *} \tag{3}$$

Thus, the experimental time is proportional to the ratio of the longitudinal T_1 and the effective transverse relaxation time T_2* of the imaging medium within the tissue. With all other conditions the same, an image with a desired signal to noise ratio could be obtained faster if T_1 is shorter and T_2* is longer.

Heterogeneity of tissue samples induces large random intrinsic magnetic field gradients,[15] which directly affects the effective transverse relaxation time and consequently, both the *SNR* and resolution.[15,16] The influence of the intrinsic field gradient can be expressed over the susceptibility gradient across the voxel $\Delta\chi$ ($\Delta\chi = \chi_{tis}^{loc} - \chi_{solv}$) as $\gamma B_0 \Delta\chi$ where γ is the gyromagnetic ratio and B_0 the external magnetic field. Then, the effective transverse relaxation rate is the sum of the intrinsic transverse relaxation rate $1/T_2$ (signal dephasing due to homogeneous line broadening) and the signal dephasing caused by the susceptibility gradients:

$$\frac{1}{T_2^*} = \frac{1}{T_2} + \gamma B_0 \Delta\chi \tag{4}$$

The additional relaxation rate term represents signal broadening across the voxel due to the differences in the magnetic susceptibilities between the tissue and the solvent and is equivalent to inhomogeneous broadening of the spectral line. The phase of the signal from individual spins varies with the spin location within a voxel, which leads to partial signal cancellation. Obviously, on the microscopic level, the magnetic susceptibilities of various tissue components are different and it is conceivable that diverse solvents with their own susceptibility could selectively modulate $\Delta\chi$ across the specimen.

Diffusion of spins within the susceptibility induced magnetic field gradient produces additional effects which depend on the diffusion rate[17] but which are of concern only at a resolution below 10 μm pixel^{-1}.[4] Here, the effects of a linear field gradient, G, applied during the imaging sequences are of more interest. Random motion (diffusion) of the spin in this gradient leads to spin dephasing which ultimately can be expressed with an additional term in the transverse relaxation rate:[3]

$$\frac{1}{T_{2\text{diff}}^*} = \frac{1}{T_2^*} + kG^2D \tag{5}$$

where D is the diffusion coefficient of the medium and k is a constant that encompasses the parameters of the specific method used to measure the relaxation (gradient echo *vs*. spin echo *vs*. CPMG). Combining expressions (2)–(5), an estimate can be obtained of the influence of the solvent properties (T_1, T_2, D and ε'') on the sensitivity per unit time in a spin echo type of experiment:

$$SNR_t = \frac{SNR}{t_T} \propto N \frac{1}{\varepsilon''^{1/2} T_1} \left(\frac{T_2}{1 + kG^2 D T_2} \right)^{3/2} \tag{6}$$

Thus, the best imaging solvent is the one with the highest spin concentration (number of equivalent spins per unit volume) N, the longest T_2, the shortest T_1 ($T_1 \geq T_2$), smallest diffusion coefficient D, and the smallest imaginary part of the dielectric permittivity, ε''.

EXPERIMENTAL METHODS

Mouse brain tissue preparation

Throughout this work, formalin-fixed paraffin-embedded (FFPE) mouse brain, prepared earlier in a standard manner was used. Briefly, mice were perfused *via* intracardiac puncture with 50 mL of 10 % neutral-buffered formalin (NBF). The brains were removed and post fixed for 24–48 h in 10 % NBF. Uniform 1 mm coronal cuts of the brain were made using brain matrix, resulting in 6 pieces that were embedded in paraffin. Mid-section (A3) was removed from the paraffin block by melting the paraffin away. The sections were deparaffinized with xylenes or Clearify (both from Electron Microscopy Sciences, Hatfield, PA) by dipping them twice into a 50 fold larger volume of the deparaffinization solvent for an hour at 60 °C. Deparaffinized specimens were similarly treated with fresh solvent and subsequently transferred into custom-made rectangular glass cuvettes, 10 mm×8 mm×1.5 mm suitable for mounting on a surface coil. For DMSO, the specimens were allowed to swell in the solvent overnight before the scanning. Solvents at hand were used: methanol, acetone and DMSO (all from Sigma) and solvents used for tissue processing for histology paraffin, xylenes and "Clearify" (all from Electron Microscopy Sciences, Hatfield, PA). The xylenes used were an *o*-, *m*- and *p*-xylene mixture, which showed two distinct groups of lines at ≈2.2 ppm (methyls) and 7 ppm (aromatics) in high-resolution ^{1}H-NMR spectra. Separation of ≈5 ppm is enough to excite selectively only one group, in this study, the methyls. Clearify is a mixture of aliphatic hydrocarbons that is used for tissue deparafinnization. In the ^{1}H-NMR spectra, three distinct groups of lines corresponding to CHs, CH_2s and CH_3s at ≈0.9, 1.3 and 1.5 ppm are visible.

Thus, the "Clearify" point spread function could be approximated with a Gaussian distribution with an intrinsic width of ≈0.6 ppm, *i.e.*, 420 Hz at 16.4 T. In solution, the paraffin ^{1}H-NMR spectrum consists of 2 sharp singlets, CH_3s at ≈0.9 ppm and CH_2s at 1.3 ppm with the ratio 1:6, which corresponds to the linear aliphatic chain CH_3–$(CH_2)_{24}$–CH_3. Although the paraffin point spread function seems to have an intrinsic width of ≈0.4 ppm, *i.e.*, 280 Hz at 16.4 T, due to the overwhelming CH_2 signal, it behaves like a real delta function (width below 10 Hz). For reference, the brain slices were also scanned while in 10 % neutral buffered formalin (NBF), which is routinely used for tissue preservation.

Magnetic resonance microscopy

A 16.4 T vertical bore spectrometer (Avance III, Bruker-Biospin, Billerica, MA) equipped with micro-imaging accessories and a temperature controlled probe head with a 10 mm surface coil was employed. The experiments were performed with a gradient coil core temperature of 21 °C, except for the paraffin studies. In the paraffin experiments, the specimen temperature was maintained at 70 °C by a stream of hot air using a temperature controller built into the spectrometer and driven by the manufacturer's software (TopSpin 2.0). The mouse brain specimens were 1–2 mm thick and were scanned with a spin–echo method using parameters optimized separately for each experiment (given in the captions of presented figures), providing 3D images with isotropic resolution of 25–64 μm pixel^{-1} for a total scanning time of 4 to 16 h.

Parametric images, T_1 and T_2, were reconstructed from a series of single slice 2D RARE scans, recorded with variable repetition and echo times, respectively. Image reconstruction was performed by curve fitting (pixel by pixel) of a respective series of images using the same software package as for the data collection (ParaVision 5.1, Bruker-Biospin).

RESULTS AND DISCUSSION

The relevant properties of the solvents used in this work are listed in Table I. The bulk solvent values were measured from the region of interest (ROI) placed into the solvent, whereas the tissue values are average values across the tissue. The solvents are listed by their polarity. Notable are the extremely low dielectric losses (ε'') in non-polar solvents, which are especially important at higher fields as dielectric losses scale with the cubic power of the resonance frequency.[13] For example, dielectric losses in water increase ten-fold on going from 500 to 950 MHz.[13] Thus, finding a suitable solvent would be of great value for high field MRM. From this point of view, the most promising solvents are hydrocarbons (paraffin, "Clearify" and xylenes) and, to some extent, acetone.

Diffusion coefficients are apparently unrelated to dielectric properties, as can be seen in Table I. The slowest diffusion was in the paraffin melt, "Clearify" and DMSO. The water signal attenuation due to diffusion is appreciable when the imaging resolution approaches 50 μm pixel^{-1}. According to Eq. (6), the signal attenuation (reciprocal of SNR_t) scales with the third power of the gradient, thus it rapidly increases with increasing resolution. As it also scales with $D^{3/2}$, slowing the diffusion at a given resolution could appreciably reduce the attenuation. For example, substituting water with DMSO could reduce the attenuation five times and with paraffin, almost twenty times, Eq. (6). Thus, paraffin and DMSO

are expected to give stronger signal than water at the highest possible resolution (25 μm pixel^{-1} in the present case).

TABLE I. NMR properties of some organic solvents

Solvent	Polarity	ε'[a]	ε''[a]	D / 10^9 m^2 s^{-1}	T_1 / ms neat/tissue[b]	T_2 / ms neat/tissue	N[c] mol L^{-1}
Paraffin[d]	Apolar	2[e] (1.9)[f]	0.001	0.32	1210/1210	220/35	128
"Clearify"	Apolar	2[e]	0.001	0.71	1180/1200	73/25	na
Xylenes	Apolar	na (2.4)[f]	na	2.3	4230/2000	40/15	49
Acetone	Polar aprotic	2	0.03	4.6	> 6000/na	na/na	81
CH_3OH	Polar protic	31	0.38	2.2	4930/2600	54/22	74
DMSO	Polar aprotic	47	0.24	0.73	2240/1500	160/20	85
NBF (H_2O)	Polar protic	79	0.2	2.3	2450/1500	16/12	111

[a]At 930 MHz[13]; [b]at 16.4 T (700 MHz); [c]proton spin concentration (mol/L) of neat solvent; [d]melt at 70 °C; [e]the *n*-hexane value; [f]CRC Handbook of Chemistry and Physics

Table I shows that all solvents have T_1 relaxation times within a factor 2 of the water (in NBF) value except for acetone, for which T_1 is impractically long. Paraffin and "Clearify" relax twice as fast as water, while DMSO has a very similar relaxation time to water; hence, from this point of view, all three solvents are good candidates.

It is well known that the water relaxation is highly accelerated by internal water chemical exchange and it is not surprising that all solvents have longer T_2 relaxation times than water. Notable is the ten-fold longer T_2 relaxation time of DMSO and the even longer one of paraffin, which puts these solvents ahead of others in terms of relative sensitivity per unit time, Eq. (6).

Finally, the last column in Table I shows molarity of equivalent spins in neat solvents. Only paraffin has somewhat higher proton concentration than water. In other solvents, concentrations are lower partly because of the lower densities of the solvents (apart from DMSO) and partly because of the much lower proton contribution to molecular mass.

The apparent superior properties of paraffin compared to water (significantly lower dielectric losses, slower diffusion, longer T_2, shorter T_1 and higher proton spin concentration) do not guarantee that it would be a better imaging solvent. Increased *SNR*, as provided by such properties, is unrelated to the image contrast that is essential for high quality images. NMR contrast originates from the local variability of NMR parameters, which in turn is caused by the tissue–solvent interaction. A simple way to estimate the strength of interactions is to compare NMR properties of neat solvents and the solvent within tissue. Such a comparison is made in Table I for the T_1 and T_2 relaxation times. Equality of the paraffin and "Clearify" T_1 relaxation times in bulk and tissue indicates the absence of an interaction between the tissue and these aliphatic solvents. Thus, T_1 contrast is negligible in these cases. However, in xylenes and methanol, the T_1 relaxation

times in tissue are half of the values in bulk solvents. Shortening of T_1 was observed also in water and DMSO, although somewhat smaller. Any reduction of the relaxation time indicates solvent–tissue interaction, which in the framework of Eq. (1) points to the presence of one or more new solvent fractions. Similarly, shortening of T_2 relaxation times, observed in all cases, points to the existence of local field fluctuation that could range from real solvent–tissue interaction (spin exchange or molecular binding) to unrestricted motion of the solvent spins in the local field gradient. In any case, the change in the relaxation time is an indicator of potential contrasting.

Representative slices from 3D T_2-weighted images in various solvents are shown in Fig. 1. The imaging conditions were different mostly because attempts were made to optimize the parameters for each solvent independently. Panel A shows a single slice of the mouse brain in water (NBF) with 32 μm pixel^{-1} isotropic resolution. Clearly visible are the dorsal hippocampus, thalamus, hypothalamus and cortex. The mice used in this study were infected with the Theiler murine encephalitis virus (TMEV), a murine multiple sclerosis (MS) model. Intracerebral TMEV infection results in chronic-progressive demyelination in susceptible mouse strains. The dark areas above the hippocampus (and below on the right) are from hemorrhages from intracerebral injections.

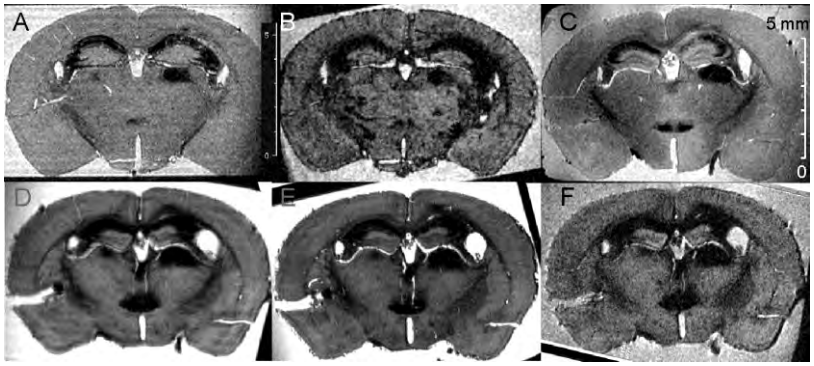

Fig. 1. Slices from 3D RARE (spin echo) scans of mouse brain in different solvents. A) H_2O (NBF): TE_{eff} 26, EncMTX 333×176×78, FOV 12.8×8×3.2, MTX 400×256×100, RareFactor 4, TR 2100, ScanTime 12 h, SpatResol 32 μm pixel^{-1} (isotropic); B) CH_3OH: TE_{eff} 26, EncMTX 166×88×50, FOV 12.8×8×3.2, MTX 200×128×64, RareFactor 4, TR 2200, ScanTime 4 h, SpatResol 64×63×50 μm pixel^{-1}; C) DMSO: TE_{eff} 11, EncMTX 333×176×78, FOV 12.8×8×3.2, MTX 400×256×100, RareFactor 1, TR 3000, ScanTime 11.5 h, SpatResol 32 μm pixel^{-1} (isotropic); D) "Clearify": TE_{eff} 26, EncMTX 333×176×100, FOV 10.2×6.4×3.2, MTX 400×256×128, RareFactor 4, TR 2200, ScanTime 16 h, SpatResol 25 μm pixel^{-1} (isotropic); E) paraffin: TE_{eff} 26, EncMTX 333×176×100, FOV 10.2×6.4×3.2, MTX 400×256×128, RareFactor 4, TR 2200, ScanTime 16 h, SpatResol 25 μm pixel^{-1} (isotropic); F) xylenes: TE_{eff} 31, EncMTX 426×220×100, FOV 12.8×8×3.2, MTX 512×320×128, RareFactor 4, TR 2400, ScanTime 14.7 h, SpatResol 25 μm pixel^{-1} (isotropic). The brightness was adjusted for each panel separately.

The methanol image, panel B, shows much better contrast but, although recorded with half the resolution, has a much lower *SNR* (owing to the longer T_1) than the water image. On the other hand the DMSO image, panel C, exhibits a much better *SNR* and contrast than the water image, most likely due to the slower diffusion and shorter T_1.

The aliphatic hydrocarbon images (D – "Clearify", E – paraffin) show superior sensitivity and contrast compared to the polar solvent images, mostly because of their much longer T_2 values. In addition, their lower diffusion coefficients enabled scanning at the even higher resolution of 25 μm pixel^{-1}. A moderate blurring in the Clearify image caused by a relatively poor point spread function should be noted. With effective spectral width of 50–100 kHz and readout size of 400 points, the Clearify signal spreads over a few pixels introducing noticeable blurring compared to the paraffin image. The xylenes image, panel F also exhibits excellent contrast, but due to long T_1 suffers from a poor *SNR*. The acetone image (not shown) was of rather poor quality partly because of an extremely long T_1 (very low *SNR*) and partly because of the volatility of the solvent (artifacts caused by the change of the sample volume (solvent is lost due to the evaporation)).

Figure 2 shows T_1 parametric images of the mouse brain slices in the indicated solvents. In polar solvents (A – water, B – methanol, C – DMSO) there is noticeable variation of T_1 within the tissue and between tissue and the solvent,

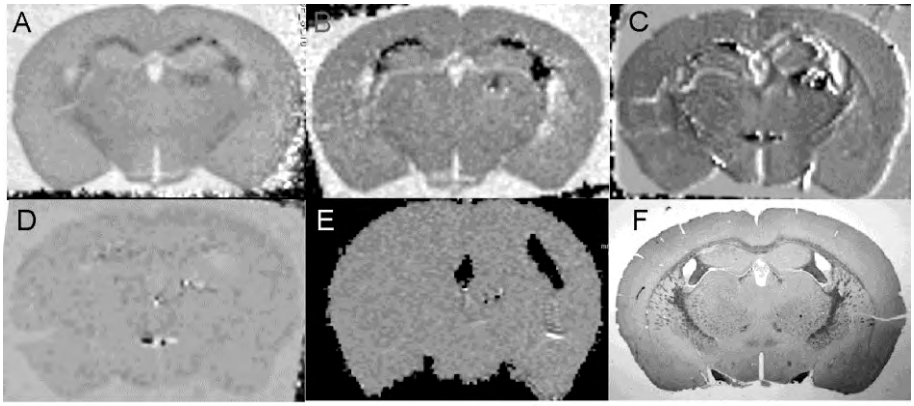

Fig. 2. Parametric T_1 images of the mouse brain slice in different solvents. A) H_2O (NFB), B) CH_3OH, C) DMSO, D) "Clearify", E) paraffin and F) optical image (1.25×) of a 5 μm slice taken from a formalin-fixed, paraffin-embedded mouse brain slice. The observed contrast depends on the tissue–solvent interaction. Notable is the complete absence of an interaction (uniform T_1 parametric image) between tissue and paraffin, panel E. The brain contour is visible because the specimen was mounted " dry" on the surface coil; otherwise, due to T_1s in tissue and bulk solvent being the same (lack of contrast), the slice would completely merge with the solvent background signal. In all other cases, the solvent T_1 was longer than the tissue T_1.

but in aliphatic hydrocarbon solvents these variations are either minimal (D – "Clearify") or nonexistent (E – paraffin). There is no background in panel E because the specimen was mounted "dry" on the surface coil. Otherwise, when immersed in paraffin, the tissue signal fuses completely with the surrounding solvents signal. This uniformity of T_1 clearly indicates that paraffin molecules do not interact with any of the tissue components, which actually could help in the interpretation of the T_2 relaxation of the paraffin in tissue (*vide infra*). Interestingly, the xylenes T_1 parametric image (not shown) is uniform within the tissue, like the paraffin image, but has an intensity distinctly different from that of the surrounding solvent.

For reference, Fig. 2F shows an optical image of a 5 μm thick paraffin-embedded slice. The NMR images can hardly match the optical ones in resolution and contrast but they are obtained from the intact paraffin block while the slice must be physically cut for optical microscopy. This opens an interesting prospect for MRM of paraffin-embedded tissue as NMR images could be used to guide sectioning of ROIs for subsequent specimen cutting for histological analysis.

Mouse brain T_2 parametric images in various solvents are shown in Fig. 3. Notable are the differences between the tissue and solvent signal in all cases. Again, the background signal in the paraffin image, panel E, is absent because the specimen was mounted "dry" on the surface coil. However, traces of bulk solvent are visible as very bright spots in the specimen cracks. Large differences in signal intensity between the solvent and tissue for hydrocarbon solvents (D – –"Clearify", E – paraffin, F – xylenes) mean that the major source of contrast is the local field gradients. For polar solvents, in addition to local gradients, other

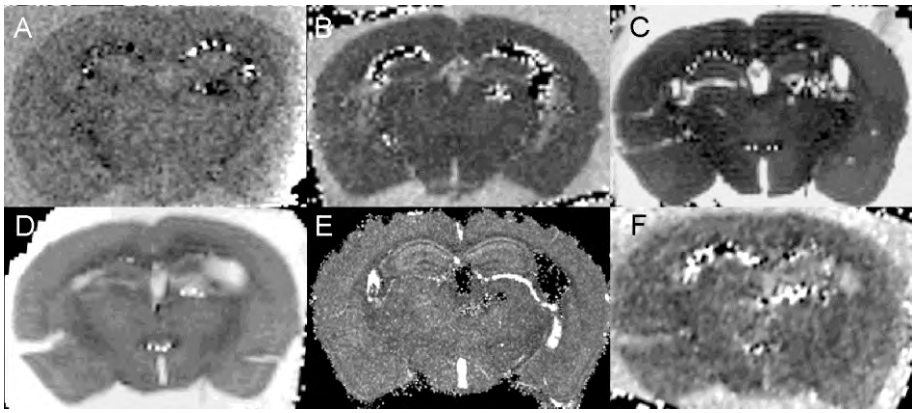

Fig. 3. Parametric T_2 images of the mouse brain slice in different solvents. A) H_2O (NFB), B) CH_3OH, C) DMSO, D) "Clearify", E) paraffin and F) xylene. Notable are the differences between the tissue solvent and bulk solvent intensities. In panel E, the background is black because the specimen was mounted 'dry'; neat solvent is visible only in the tissue pockets (white areas).

interactions may exist, such as chemical exchange with tissue labile protons (water, methanol) or binding (adsorption, absorption and intercalation) of solvent molecules in the tissue matrix (water, methanol and DMSO).

One way to test the existence of an interaction between the solvent and tissue is to monitor magnetization exchange between the two components of the solvent mixture. In high resolution spectroscopy this experiment is known as ILOE[11] and in NMR imaging as magnetization transfer (MT).[18] Both experiments are based on incoherent magnetization exchange (chemical exchange and cross-relaxation[12,19,20]), the only difference being whether the transferred magnetization is used to modulate the image or high resolution spectrum. Briefly, while a resonance line at one frequency is observed, the other frequency or frequency band is irradiated. Irradiation saturates the lines at the selected resonances. In the presence of magnetization exchange, this saturation is transferred to exchanging partners causing a signal decrease at the observed line. Intermolecular chemical exchange involves labile protons and is not of concern here. More interesting is cross-relaxation which depends on both the geometry and mobility of the interacting nuclei.[12] At the spin-diffusion limit ($\omega_0\tau_c > 1$, ω_0 – resonance frequency, τ_c – correlation time), the cross-relaxation rate is proportional to the correlation time: the longer the correlation time, the higher the rate. At the other limit, extreme narrowing ($\omega_0\tau_c < 1$,) results in cross-relaxation being significantly lower and of the opposite sign.[12] Thus, strong intermolecular cross-relaxation indicates that the observed spin pair is in the spin diffusion regime, which at 700 MHz would mean that the two spins are in close proximity for longer than 0.3 ns. This time interval is about three orders of magnitude longer than the correlation time in free liquids (≈1 ps). In other words, observation of strong intermolecular magnetization transfer between small molecules indicates their binding on a common substrate. In the present case, observation of MT in a mixed solvent would indicate solvent–tissue interaction. To test for solvent–tissue interaction, a mixture of water and DMSO was selected. From the ^{1}H-NMR spectrum of DMSO around the tissue (not shown), it was found that the solvent contained ≈20 % water (the water signal was ≈15 % of the total magnetization and ≈900 Hz downfield from the DMSO signal); thus the original DMSO specimen without any changes was used as a mixed solvent system.

The Z-spectrum obtained by systematic irradiation of the 8 kHz range around the DMSO resonance, in increments of 200 Hz, is shown in Fig. 4. A single slice FLASH image was generated by selective excitation and detection of the DMSO line was conducted where, in a series of experiments, the irradiation frequency was systematically changed from one experiment to another. Three ROIs were selected: within the tissue (thalamus), within the solvent (bulk) and outside tissue and solvent (the noise floor). The frequency offset was counted from the DMSO resonance that was solely detected. In the bulk solvent, only

direct saturation around zero offset exists: the observed resonance line is hit directly by the saturating field that resulted in a massive signal reduction. Thus, in neat mixed solvent, no MT was detected. However, within the tissue manifest MT between water and DMSO was observed. A minimum at ≈1 kHz (water resonance) showed that the DMSO signal is significantly reduced when the water line is saturated, indicating strong cross-relaxation between the water and DMSO proton spins. Strong cross-relaxation could be observed only if both molecules reside within the tissue for longer than 0.3 ns, which could be interpreted as solvent binding. In the present case, the MT effect was uniform across the tissue and besides binding no new information was added. However, it is conceivable that in different solvent mixtures and in a different tissue, the ILOE could exhibit regional selectivity, which could be an additional useful contrasting tool.

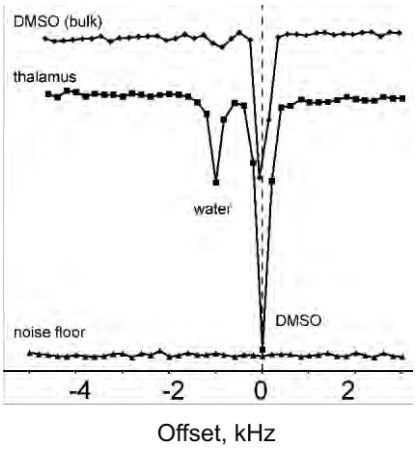

Fig. 4. The Z-spectrum of the DMSO–water system. Magnetization transfer was performed in a series of 41 2D FLASH experiments with MT offsets from –5000 to +3000 Hz (in 200 Hz increments). The offset was measured from the DMSO resonance that was selectively detected and used to generate the images. In a single experiment, saturation was performed with a series of 20 Gaussian pulses, 10 ms with MT time 200 ms and 1 μT amplitude, which kept a saturation bandwidth of 275 Hz. The points represent the signal integral from the indicated region of interest at a given offset.

CONCLUSIONS

It was shown that the MRM of tissue in organic and mixed solvents is a promising approach for improvement of image quality and for a better understanding of tissue–solvent interactions. The employment of organic solvents for MRM at high fields is particularly promising because aliphatic solvents eliminate some of the problems encountered in standard imaging using water. The properties of an ideal MRM solvent were briefly discussed and a few available in the lab were tested experimentally. It was found that the most promising of these were paraffin (at 70 °C) and DMSO, but, with certainty, there are some further options that could be even better. In addition, the use of mixed solvents was proposed, and experimentally demonstrated, as a means to test the residence time of solvent molecules on the tissue surface.

Acknowledgement. We thank Mr. David Hinton for critical reading of the manuscript.

ИЗВОД

NMR СЛИКАЊЕ ТКИВА У ОРГАНСКИМ И МЕШОВИТИМ РАСТВАРАЧИМА

SLOBODAN MACURA[1], PRASANNA K. MISHRA[1], JEFFREY D. GAMEZ[2] и ISTVAN PIRKO[2]

[1]Department of Biochemistry and Molecular Biology и [2]Department of Neurology, Mayo Clinic, Rochester, Minnesota, 55905, USA

У овом раду разматрана је употреба органских и мешовитих растварача за нуклеарно-магнетно-резонантну микроскопију фиксираних ткива, као средства за побољшање информационог садржаја NMR слике. NMR својства неких стандардних растварача (метанол, ацетон и диметил-сулфоксид (DMSO)) и растварача који се користе за обраду ткива у патологији (ксилен, парафин и „*Clearify*“) измерени су, прегледани и анализирани. Утврђено је да су DMSO и парафин веома корисни растварачи који пружају слике бољег квалитета од оних добијених у води (неутралном формалинском пуферу). Ово је илустровано на узорцима формалином фиксираног мишјег мозга сликаног на 16,4 T (700 MHz).

(Примљено 8. октобра 2013)

REFERENCES

1. P. C. Lauterbur, *Nature* **242** (1973) 190
2. A. Kumar, D. Welti, R. R. Ernst, *J. Magn. Reson*. **18** (1975) 69
3. E. M. Haacke, *Magnetic resonance imaging: physical principles and sequence design*. Wiley, New York, 1999.
4. P. T. Callaghan, *Principles of nuclear magnetic resonance microscopy*. Oxford University Press/Clarendon Press, Oxford (England)/ New York, 1991
5. P. Caravan, J. J. Ellison, T. J. McMurry, R. B. Lauffer, *Chem. Rev*. **99** (1999) 2293
6. T. M. Shaw, R. H. Elsken, *J. Chem. Phys.* **21** (1953) 565
7. K. Venu, V. P. Denisov, B. Halle, *J. Am. Chem. Soc.* **119** (1997) 3122
8. B. Halle, *Magn. Reson. Med.* **56** (2006) 60
9. P. S. Belton, *Cell. Mol. Life Sci.* **57** (2000) 993
10. R. A. Brooks, F. Moiny, P. Gillis, *Magn. Reson. Med.* **45** (2001) 1014
11. D. Li, E. DeRose, R. London, *J. Biomol. NMR* **15** (1999) 71
12. S. Macura, R. R. Ernst, *Mol. Phys*. **41** (1980) 95
13. T. Horiuchi, M. Takahashi, J. Kikuchi, S. Yokoyama, H. Maeda, *J. Magn. Reson*. **174** (2005) 34
14. S. Blackband, D. Buckley, J. Bui, M. I. Phillips, *MAGMA* **9** (1999) 112
15. R. J. Kurland, F. Q. H. Ngo, *Magn. Reson. Med.* **3** (1986) 425
16. J. A. Glasel, K. H. Lee, *J. Am. Chem. Soc.* **96** (1974) 9
17. R. P. Kennan, J. Zhong, J. C. Gore, *Magn. Reson. Med.* **31** (1994) 9
18. S. D. Wolff, R. S. Balaban, *Magn. Reson. Med.* **10** (1989) 135
19. S. Macura, R. R. Ernst, *Period. Biol*. **83** (1981) 87
20. S. Macura, W. M. Westler, J. L. Markley, *Methods Enzymol* **239** (1994) 106.